SEMARAK ILMU PUBLISHING

Journal of Advanced Research in Applied Sciences and Engineering Technology

Journal homepage:
https://semarakilmu.com.my/journals/index.php/applied_sciences_eng_tech/index
ISSN: 2462-1943

Multi-Weld Quality Optimization of Gas Tungsten Arc Welding for Aluminium 6061 using the Grey Relation Analysis-Based Taguchi Method

Ibrahim Sabry[1,*], A.M. Hewidy[1]

[1] Department of Mechanical Engineering, Faculty of Engineering, Benha University, Benha, 13511, Egypt

ARTICLE INFO

Article history:
Received 18 August 2023
Received in revised form 7 October 2023
Accepted 7 November 2023
Available online 25 December 2023

Keywords:

TIG; Al 6061; L9 Taguchi; Hybrid Grey-Taguchi; Multi-performance characteristics

ABSTRACT

The optimization of parameters is crucial in the joining process, particularly in welding, to attain connections with exceptional mechanical properties. In the present study, the welding of aluminium 6061 was conducted with a TIG, an acronym for tungsten inert gas, is formally referred to as gas tungsten arc welding (GTAW) technique, employing a suitable ER 4043 electrode and argon shielding gas. The investigation of optimal welding parameters, specifically current, voltage, and flow rate, is conducted utilizing statistical methodologies such as the hybrid Grey-based Taguchi process. The desired attributes for high-quality welds were established as having high tensile strength, hardness, and a low rate of corrosion. Given the presence of three responses and one objective, the hybrid Grey-based Taguchi method is employed. The statistical approaches have converged on optimal parameters of 120 A, 20 V, and 15 L/min. The present analysis reveals that the ideal welded junction exhibited the following characteristics: a tensile strength of 190.169 MPa, a hardness value of 77HV, and a corrosion rate of 0.29 mm. The current parameter was found to have the highest contribution, accounting for 65.66% of the overall performance of the weldments. Confirmatory testing was conducted in order to confirm the optimization strategy, and the findings indicated that the Grey-based Taguchi technique is a straightforward yet effective approach for optimizing welded connections across several performance criteria.

1. Introduction

Welding is the technique that enables the joining of various materials, for instance, metals, polymers, and alloys, by carefully regulated heat under pressure or without it. When controlled heat is applied at the interface, the materials initially tend to melt, and a permanent joint is established after solidifying the molten material there [1]. The joining procedure involves melting the opposing components with a heat source and solidifying them to create a permanent joint with a strength that is at least as strong as the parent metal. Depending on the thickness of the metal sheet to be welded, welding can be done with or without the inclusion of filler material and provides a solid connection between the welded joints. Any material's capacity to be bonded by welding depends on the

* *Corresponding author.*
E-mail address: Ibrahim.sabry@bhit.bu.edu.eg

https://doi.org/10.37934/araset.36.1.2642

metallurgical phenomenon that occurs during the welding process and results in numerous changes to a wide range of material properties. The aerospace, spacecraft, structural, and military industries all use aluminium alloys as their preferred material [2]. Depending on the type of material chosen and the joint's intended application, the joint may be produced using flux or filler material. The inert gases (helium, argon, or a mixture of helium and argon) are frequently employed to cover the area welded from the atmosphere [3]. It is also possible to manually feed filler metal for proper welding. The TIG welding procedure, sometimes called GTAW, was created during World War II. The development of the TIG welding method has increased the likelihood of joining materials that are more difficult to join, such as aluminium and magnesium. Numerous ways can be used to weld thick aluminium alloy plates [4].

Nevertheless, because arc welding uses less energy and offers more flexibility, like GMAW and TIG welding, it is a more affordable choice [5]. Welding thick plates of Al alloys is a severe problem because fusion welding can cause pore flaws [6]. In the current experiment, mild steel plate temperatures of zero and thirty degrees Celsius are used to evaluate the heat generation during submerged arc welding on the plate. The feasibility of submerged arc welding at zero degrees Celsius for the plate has been established [7]

Specific characteristics of aluminium alloys include a higher elastic modulus, a high specific strength, exceptional fracture toughness, and superior corrosion resistance [8]. During heat treatment, precipitation hardening and phase transformation increase the strength of 6061 aluminium alloys (6061). These alloys can also be used for welding. It is a precipitation-hardened aluminium alloy with silicon and magnesium as key alloying components. It was created in 1935 under the designation Alloy 61S [9]. The most frequently used dissimilar alloys for broader applications demonstrate good mechanical and weldability features. TIG welding involves heating the joining metals using an arc created by a non-consumable electrode and parent metal through coalescence. TIG is the generality utilized joining technique for welding Al-6061 alloys [10]. The TIG joining process uses various techniques, including pulsing and magnetic arc oscillation. TIG welding has been used extensively for numerous projects using various aluminium alloys. Using pulsed TIG welding, Gaurav Sharma *et al.,* [11] investigated the joining aluminium alloys' thick plates (6 mm thickness). They noticed that the shear strength changes depending on the pulse current and whether there are pores in the weld zone. Weld joint shear strength was determined to be 73 MPa, compared to 85 MPa for parent metals. In order to manage the speed of welding for satisfactory joints, Praveen et *al.,* [12] examined the automatic TIG welding of Al-5083 utilizing a filler rod of Al-5356. They explored how welding current and speed affected the mechanical properties of the welded joint, including its UTS and VHN. Indira Rani *et al.,* [10] investigated the TIG welding of Al-6351 alloy to examine the welded junction's mechanical attributes. They investigated how pulse and non-pulse current affected weldability and discovered that the UTS of the weldments was equivalent to that of the B.M. Also noted was the failure of the tensile samples in the HAZ region.

The TIG welded junction of AA 6082 has typically had a higher strength than the MIG welded joint. Because of the narrower arm spacing, the grain structure was more evenly distributed and had a higher tensile strength. Additionally, the electrode's travel speed directly impacts the phenomenon of welding region softening. Aging at 0°C has led to an increase in the weld's hardness [13]. A double-side V butt weld junction was made using two separate filler materials, AA 4043 and AA 4047. When argon is used as a shielding gas, and the current increases from 80 Amp to 120 Amp, the tensile strength typically rises by 4.5%. The outcomes are improved when AA 4043 is utilized rather than AA 4047. The weld zone's front breadth and height, which dictates its geometry, determine the superiority of a TIG weld [14-16].

Dipankar Dey *et al.,* [14] According to the Grey-Taguchi technique, the optimal parametric combination consists of a weight percent reinforcement of 9%, a load of 10 newtons, a sliding velocity of 2 m/s, and a sliding distance of 1000 m. The confirmation experiment validates the optimal parametric combination by assessing its grey relational grade, determined by its ranking. Based on the obtained results, it can be extrapolated that the Grey-Taguchi approach is a valuable tool in improving the tribological performance of Al2024-TiB2 composites. Dipankar Dey *et al.,* [15] The multi-objective optimization problem is transformed into a single-objective optimization by applying grey-fuzzy analysis. Based on the grey-fuzzy analysis, the optimal combination of tribological parameters is L1S4D2, which corresponds to a load of 10N, a sliding speed of 2.0 m/s, and a sliding distance of 1000 m. An additional confirmatory experiment has been employed to authenticate the optimal set of parameters. The analysis of variance (ANOVA) results indicate that the sliding distance component has the most significant impact on the tribological performance of grey fuzzy grade. From the literature review that was previously looked at, it was found that very little work has been done in the past to combine Al–6061 alloys utilizing TIG welding in a butt joint configuration. This study aims to enhance the TIG welding process parameters through the application of hybrid GRA, utilizing the Taguchi method. The investigation focuses on the butt joint welding of Aluminium 6061, with an emphasis on evaluating the UTS, C.R., and VHN.

2. Material and Methodology

2.1 Selection of Material

Aluminium 6061 plates 5 mm thick with a 2.5 mm groove butt junction were the materials employed in this study. The filler material was ER4043 wire, 1.6 mm in thickness. The molten metal is due to silicon's inclusion in the welding wire. B.M. chemical compositions and mechanical characteristics are provided 6061in Tables 1 and 2, respectively. The shielding gas was a combination of argon and carbon dioxide.

Table 1
Shows the aluminium 6061 composition of chemicals

Weight %	6061
Al	Ball
Si	0.4
Fe	0.70
Cu	0.15
Min	0.15
Mg	0.9
Cr	0.04
Zn	0.25
Ti	0.15

Table 2
Shows the aluminium's mechanical characteristics in 6061

Weight %	6061
σ UTS M pa	252.690
EL%	8
VHD	86

2.2 Parameter Selection for the Welding Process

Based on earlier research [16], the process parameters and their values were selected. For the L9 Taguchi orthogonal array, A, V, and F at three levels were chosen. Table 3 lists the parameters and their levels.

Table 3
The levels of the parameters used in the welding process

Parameters of Process	Unit	Symbol	Levels		
			-1	0	1
Amper	A	A	105	110	115
volt	V	v	17	18	19
Flow rate	(L/min)	F	10	15	17

2.3 The Machine is Welded

Using a can weld Pulse D Series TIG welding equipment, the metal plates at the butt joint were double-sided TIG welded, as shown in Figure 1(a), Figure 1(b) illustrates the TIG welding technique applied to an aluminium alloy 6061, resulting in a welded joint.

a b

Fig. 1. TIG welding apparatus, (b) A sample of TIG-welded Al 6061

2.4 Mechanical Characteristics of the Welded Sample

The study's output responses for multi-performance optimization include the weld joints' UTS, VHN, and corrosion rate. A QT-6100 series tensile testing equipment was used to determine the tensile characteristics (Figure 2). Waterjet machining was used to separate the ASTM-E8 test specimens from the welded samples [17]. The tensile test was conducted three times for each line of the Taguchi orthogonal array, with the average being obtained each time.

Fig. 2. The apparatus used for conducting tensile testing

Figure 3 displays the tensile test sample. Everything is measured in millimetres.

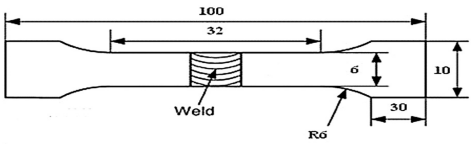

Fig. 3. A test specimen for ASTM-E8

In Figure 4, the shattered samples following the tensile test are depicted.

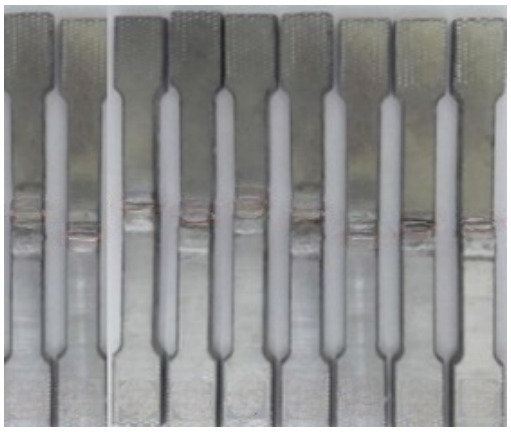

Fig. 4. Shows the broken tensile specimens

Using the hardness testing machine depicted in Figure 5, a specimen size of 20 10 mm was used to determine the VHN of the weld zone following ASTM standard E384. Standard metallographic sample preparation procedures were performed to provide a smooth surface for the hardness test. The surfaces were mechanically ground until smooth using abrasive silicon carbide papers with grit sizes ranging from 200 to 4000. The transverse portion of the weld bead was exposed on the samples when hotly mounted on poly fast resin for handling. The hardness test was conducted using the following parameters: 500 gf of indentation force, 10 seconds of dwell duration, and 1 mm of space between indentation. Multiple indentations on the weld zone were made for each line of the experiment, and the average was used to calculate the hardness value.

Fig. 5. Machine for measuring microhardness

3. Method of Optimization

3.1 Taguchi Technique

As a statistician and engineer, Taguchi is a Japanese quality manager [18]. It has been applied in various academic subjects since its invention to optimize numerous procedures. The signal-to-noise ratio is optimized by comparing those aspects of the process that can be managed—the signal—to those that cannot be controlled. Three conventional signal-to-noise ratios (S/N ratios), as shown in Eq. (1), Eq. (2) and Eq. (3) [24-28], are frequently utilized according to the required output response. The Taguchi standard orthogonal array is a technique that can acquire the optimal setup of the input process parameters with minor experimentation. Time and money are saved because fewer experiments are required to find the optimal configuration that would result in the best-required output instead of testing out all possible incorporation of the input process parameters, as is the case with the traditional experiment design [19]. The number of experiments that must be carried out is denoted by the notation La (Xn) in the Taguchi method. Where [20] is the total number of experimental runs, [n] is the total number of input process parameter levels, and [X] is the total number of levels of input process parameter inputs.

i. The 'nominal is best' signal-to-noise ratio

$$\eta = 10\ log \frac{1}{n} \sum_{i=1}^{n} \frac{\mu^2}{\sigma^2} \tag{1}$$

ii. The better the signal-to-noise ratio, the smaller

$$\eta = -10\ log \frac{1}{n} \sum_{i=1}^{n} y_i^2 \tag{2}$$

iii. "Larger is better" in terms of signal-to-noise ratio

$$\eta = -10\ log \frac{1}{n} \sum_{i=1}^{n} \frac{1}{y_i^2} \tag{3}$$

The notation provides information on the Ƞ signal-to-noise ratio, the number of experiments, the mean signal-to-noise ratio, the deviation of standard, and the output response. y_i. The optimum parameter combination is thought to have the maximum signal-to-noise ratio. Identification of the process performance/characteristics to be maximized, minimized, or maintained, identification of the performance-controlling factors, selection of the appropriate orthogonal array, execution of experimental trials to acquire output responses, analysis of the output response values to identify the optimal setting, and confirmation of the optimal setting are the steps involved in Taguchi optimization. Two of the current study's three performance traits for welding A, V, and F are the UTS and VHN of the similar butt joint. Using the Minitab 17 program, the Taguchi analysis was performed on the L9 orthogonal array. Table 4 presents the orthogonal array.

Table 4
Shows an orthogonal L9 Taguchi array

Run No	Design matrix			Estimated Mechanical parameters		
	A	V	F	UTS	VHN	CR
1	100	17	10	140.223	75.0634	0.030
2	100	19	15	138.862	74.9840	0.026
3	100	20	17	164.501	74.2501	0.029
4	110	17	15	140.223	74.9574	0.040
5	110	19	17	148.862	74.8935	0.030
6	110	20	10	144.501	75.8720	0.035
7	120	17	17	126.891	76.3654	0.024
8	120	19	10	142.530	74.8969	0.028
9	120	20	15	126.891	0.019	0.029

3.2 Grey-Relational Analysis

Real-world situations in which process performance is determined only by one objective or set of attributes are uncommon. Unfortunately, the traditional Taguchi approach is only helpful for one performance feature. This has motivated scholars to look at several options to satisfy this demand. Due to its applicability for optimizing multiple performance criteria, GRA has attracted much attention since its introduction. GRA can combine many process performance attributes into a single grey-relational grade (GRG), even though each performance feature has a specific optimal setting [24-29]. The grey-relational generation is the method behind this. The steps involved in GRA are as follows: identifying the process performance/characteristics to be maximum, minimized, or maintained; identifying the performance-controlling factors; selecting the appropriate orthogonal array; conducting the experimental trials to obtain the output response values; normalizing the output response values based on the signal-to-noise ratio criterion; computing the variation succession; and computing the threshold.

3.3 The Suggested Hybrid Approach

The Taguchi method and the GRA are combined to create the hybrid method proposed in this work. The Grey-based Taguchi method is the name given to this approach. The steps below were performed [21] After the S/N ratios of the output response values were calculated, as shown in Figure 6.

Using the major influence plots of the GRG versus the input process parameters, the Taguchi analysis is used in this flow chart in Figure 6 at step 5 to determine the optimal configuration. The output response used in this investigation is the GRG.

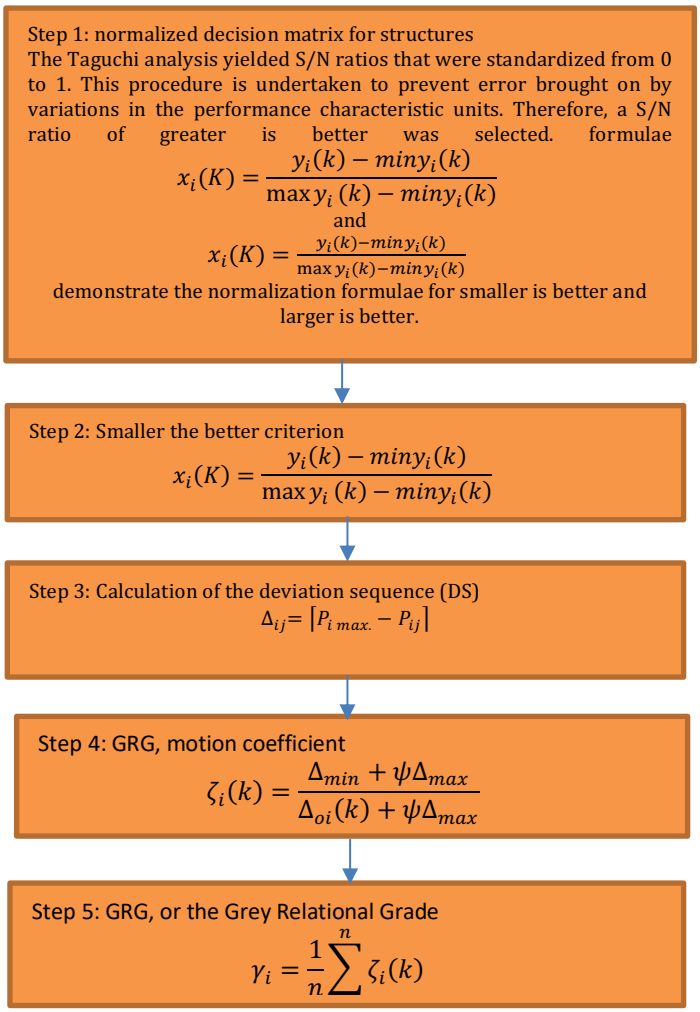

Fig. 6. Shows a step-by-step technique for applying the Grey-based Taguchi methodology

4. Results and Analysis

4.1 Mechanical Testing

Figure 7 displays the tensile parameters of the Al 6061 conventional TIG welding technique weldment, including the UTS and the location of the fracture. S1-140.223, S2-138.862, S3-164.501, S4- 140.223, S5- 148.862, S6- 174.501, S7- 126.891, S8- 142.53, and S9- 190.169 MPa were discovered to be the average UTS values for Al 6061 weldments. The UTS of the fracture, even though it occurred in the weld region, is higher than the recommended level. This demonstrates excellent joint efficiency and superb welding quality. Specimen S9 exhibits better UTS display than S3 and S6, as shown in the figure.

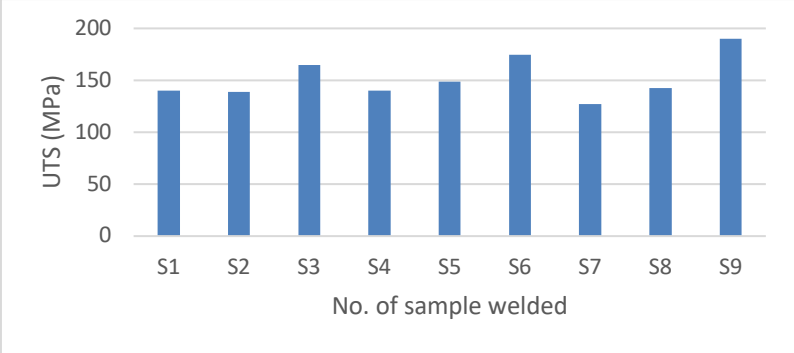

Fig. 7. Ultimate tensile strength behaviour of Al 6061at different parameters

A microhardness analysis was conducted to assess the mechanical properties of various regions inside the weld joint. Firstly, it is imperative to acknowledge that the original alloy Al 6061 exhibited an average hardness of 86 H.V. for the base metal. Conversely, an analysis of the hardness profile reveals a reduction in hardness within the weld region. This observation was made by conducting hardness measurements in different weld regions utilizing a Vickers diamond indenter. Promote the nucleation and development of all precipitates. The observed decrease in hardness at the transition area can be attributed to coarsening precipitates. The hardness values in various regions of the welded workpiece are presented in the following table. The Vickers hardness measurements conducted on the tested metals in the weld joint zone are presented in Figure 8.

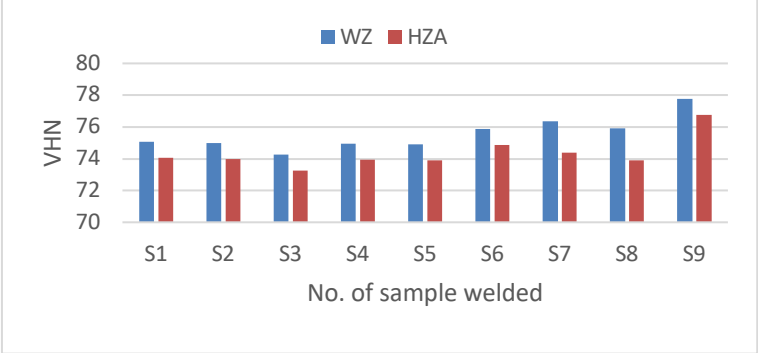

Fig. 8. Vickers hardness behaviour of Al 6061at different parameters

4.2 Experimental Findings

According to Table 4, the maximum UTS was 190 MPa, at the A of 120 amperes, V of 17 Volte, and F of 15 L/min. The maximum VHN was 77.7.65 HV at the welding current of 120 A, voltage of 20 V, and F of 15 L/min. Using the more prominent is, the better criterion, and Table 5 shows the signal-to-noise ratios of the experimental data. Figure 9 displays the primary effect graphs for each output response. Level 3 (A3V3F2) A, V, and F are the best settings for UTS. That entails an A of 120 ampers, V of 17 Volte, and F of 15 l/min, respectively. While for VHN, the ideal welding parameters are 120 A, 20 V, and 15 L/min of gas flow (A3V3F2). In contrast, the ideal welding parameters for corrosion rate are 110 A of welding current, 17 V of welding voltage, and F of 15 L/min (A2V1F2). In addition, the input process parameters affect the output responses that are both rising and decreasing, except for the UTS, which increased as the voltage climbed.

Table 5
Lists the welding settings and the experimental values' signal-to-noise ratios

Run No	Design matrix			Estimated Mechanical parameters		
	A	V	F	UTS	VHN	CR
1	100	17	10	42.9364	37.5086	30.4576
2	100	19	15	42.8517	37.4994	31.7005
3	100	20	17	44.3234	37.4139	30.7520
4	110	17	15	42.9364	37.4963	27.9588
5	110	19	17	43.4557	37.4889	30.4576
6	110	20	10	44.8360	37.6016	29.1186
7	120	17	17	42.0686	37.6579	32.3958
8	120	19	10	43.0781	37.6045	31.0568
9	120	20	15	45.5828	37.8163	30.7520

The main effects charts in Figure 9 show how process parameters affect mechanical qualities like tensile strength. Tensile strength decreased from 100 A to 110 A as the welding current increased, but it then dramatically increased to 120 A. However, as the welding voltage grew, its influence on the UTS increased. At the same time, the relation between the gas flow rate and UTS followed a pattern resembling that of the welding current. In addition, the primary effect charts in Figure 7 show that the process factors' effect on hardness differs from the trend on UTS. The interactions between the three process variables demonstrate that a better VHN property was produced by an A of 120 ampers, a V of 20 volts, and an F of 15 L/min. While a 110 A welding current, a 19 V welding voltage, and a 15 L/min gas flow rate produced higher C.R. characteristics.

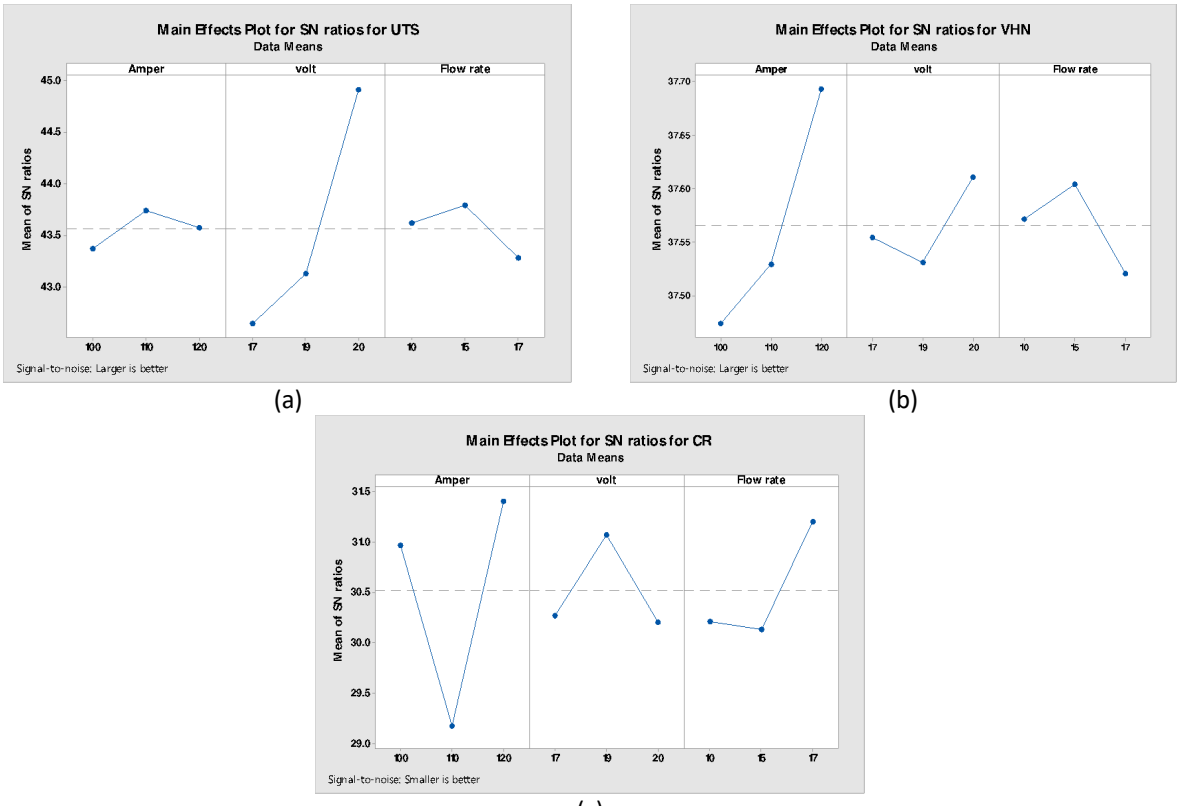

Fig. 9. shows the output responses' main effect charts(a) UTS (b) VHN (c) CR

4.3 Analysis of Regression

It is possible to express the response (Y), which includes the tensile strength (UTS), weld zone hardness (WHN), and friction rate (C.R.) of the joints, as functions of current (A), volt (V), and flow rate (F).

$$Y = f(A, V, F) \quad (4)$$

The established mathematical model equations Eq. (5), Eq. (6) and Eq. (7) are provided below for the three factors mentioned above.

$$\begin{aligned} UTS = {} & 132.3 + 0.0\ Amper\_100 + 6.67\ Amper\_110 + 5.33\ Amper\_120 + 0.0\ volt\_17 + 7.64\ volt\_19 \\ & + 40.61\ volt\_20 + 0.0\ Flow\ rate\_10 + 4.00\ Flow\ rate\_15 - 5.67\ Flow\ rate\_17 \end{aligned} \quad (5)$$

$$\begin{aligned} VHN = {} & 74.716 + 0.0\ Amper\_100 + 0.475\ Amper\_110 + 1.912\ Amper\_120 + 0.0\ volt\_17 \\ & - 0.204\ volt\_19 + 0.502\ volt\_20 + 0.0\ Flow\ rate\_10 + 0.293\ Flow\ rate\_15 \\ & - 0.441\ Flow\ rate\_17 \end{aligned} \quad (6)$$

$$\begin{aligned} CR = {} & 0.03044 + 0.0\ Amper\_100 + 0.00667\ Amper\_110 - 0.00133\ Amper\_120 + 0.0\ volt\_17 \\ & - 0.00333\ volt\_19 - 0.00033\ volt\_20 + 0.0\ Flow\ rate\_10 + 0.00067\ Flow\ rate\_15 \\ & - 0.00333\ Flow\ rate\_17 \end{aligned} \quad (7)$$

The analysis of variance technique (ANOVA) was then used to see whether the constructed models were adequate. In Tables 6, 7, and 8, respectively, the analysis of variance (ANOVA) results for UTS, hardness, and corrosion rate are presented.

Table 6
ANOVA table of UTS

Source	DF	Adj S.S.	Adj MS	F-Value	P-Value
Regression	6	3011.04	501.84	3.48	0.0240
Amper	2	74.68	37.34	0.26	0.0794
volt	2	2794.81	1397.40	9.70	0.0093
Flow rate	2	141.56	70.78	0.49	0.0671
Error	2	288.22	144.11		
Total	8	3299.26			

Table 7
ANOVA table of VHN

Source	DF	Adj S.S.	Adj MS	F-Value	P-Value
Regression	6	7.5581	1.2597	1.95	0.0377
Amper	2	5.9456	2.9728	4.61	0.0178
volt	2	0.7926	0.3963	0.61	0.0620
Flow rate	2	0.8199	0.4100	0.64	0.0612
Error	2	1.2911	0.6455		
Total	8	8.8492			

Table 8
ANOVA table of C.R.

Source	DF	Adj S.S.	Adj MS	F-Value	P-Value
Regression	6	0.000158	0.000026	2.12	0.0355
Amper	2	0.000110	0.000055	4.43	0.0184
volt	2	0.000020	0.000010	0.81	0.0552
Flow rate	2	0.000028	0.000014	1.11	0.0475
Error	2	0.000025	0.000012		
Total	8	0.000183			

4.4 Conformity Test

The researchers conducted experiments in order to validate the regression Eq. (5), Eq. (6), and Eq. (7). Nine joints were manufactured, employing varying amounts of current, voltage, and flow rate that deviated from those specified in the design matrix (Table 4). The test results are displayed in Table 9, revealing a strong concurrence between the experimental and projected values.

Table 9
Conformity test results

Run	Design matrix			Percentage error from the model prediction								
No	A	V	F	UTS	UTS(p)	Error%	VHN	VHN(p)	Error%	CR	CR(p)	Error%
1	100	17	10	140.22	139.334	1.88889	74.2501	74.7156	0.347748	0.029	0.0304444	-0.0004
2	100	19	15	138.862	140.973	2.11111	74.9574	74.8050	0.178948	0.040	0.0277778	-0.001
3	100	20	17	164.501	167.279	2.77778	74.8935	74.7768	0.526696	0.030	0.0267778	0.0022
4	110	17	15	140.223	143.001	2.77778	75.8720	75.4841	0.526696	0.03	0.0377778	0.00222
5	110	19	17	148.862	147.973	1.88889	76.3654	74.5458	0.347748	0.02	0.0304444	-0.0004
6	110	20	10	174.501	173.612	1.11111	75.8969	75.6930	0.178948	0.02	0.0367778	-0.001
7	120	17	17	126.891	125.002	2.11111	77.770	76.1865	0.178948	0.02	0.0257778	0.00177
8	120	19	10	142.530	141.308	1.77778	74.2501	76.4236	0.526696	0.029	0.0257778	0.0022
9	120	20	15	190.16	189.28	1.8888	74.957	77.423	0.34774	0.04	0.029444	0.0004

4.5 The GRA- Taguchi Method's Findings

The normalized S/N ratios, deviation sequences, GRC, GRG, and rank are shown in Tables 10, Table 11, Table 12, and Table 13 in that order.

Table 10
Presented the output responses' normalized S/N ratios

Run No	A	V	F	UTS	VHN	CR
1	100	17	10	0.01023079	0.99603336	0.05988235
2	100	19	15	0.00923223	0.99578893	0.02148189
3	100	20	17	0.0265826	0.99351735	0.05078661
4	110	17	15	0.01023079	0.99570657	0.13708491
5	110	19	17	0.01635299	0.99550996	0.05988235
6	110	20	10	0.03262582	0.99850421	0.1012519
7	120	17	17	0	1	0
8	120	19	10	0.01190134	0.99858126	0.04136955
9	120	20	15	1	0	1

Table 11
The output replies' deviation sequences' normalized S/N ratios

Run No	A	V	F	UTS	VHN	CR
1	100	17	10	0.989769	0.003967	0.940118
2	100	19	15	0.990768	0.004211	0.978518
3	100	20	17	0.973417	0.006483	0.949213
4	110	17	15	0.989769	0.004293	0.862915
5	110	19	17	0.983647	0.00449	0.940118
6	110	20	10	0.967374	0.001496	0.898748
7	120	17	17	1	0	1
8	120	19	10	0.988099	0.001419	0.95863
9	120	20	15	0	1	0

Table 12
Shows the GRC for the output responses' normalized S/N ratios

Run No	A	V	F	UTS	VHN	CR
1	100	17	10	0.335622	0.992129	0.347194
2	100	19	15	0.335398	0.991648	0.338176
3	100	20	17	0.339347	0.987201	0.345015
4	110	17	15	0.335622	0.991486	0.366861
5	110	19	17	0.337007	0.9911	0.347194
6	110	20	10	0.340745	0.997017	0.357463
7	120	17	17	0.333333	1	0.333333
8	120	19	10	0.335999	0.997171	0.342787
9	120	20	15	1	0.333333	1

Table 13
Shows the GRG and the output replies' rankings

Run No	A	V	F	GRG	RANK
1	100	17	10	0.521245	5
2	100	19	15	0.516886	8
3	100	20	17	0.519865	7
4	110	17	15	0.530159	2
5	110	19	17	0.521327	4
6	110	20	10	0.528682	3
7	120	17	17	0.516397	9
8	120	19	10	0.520692	6
9	120	20	15	0.816936	1

The highest grey-relational grade for experiment run 9 was 0.816936, as shown in Table 9. At this position, the A, V, and F are 120 A, 20 V, and 15 L/min, respectively. Figure 10 displays the GRG's central effect plot for the input process parameters. It can be demonstrated that A3V3F2 is the ideal configuration for the multiple performance characteristics of the TIG butt joint (UTS, VHN, and C.R.).

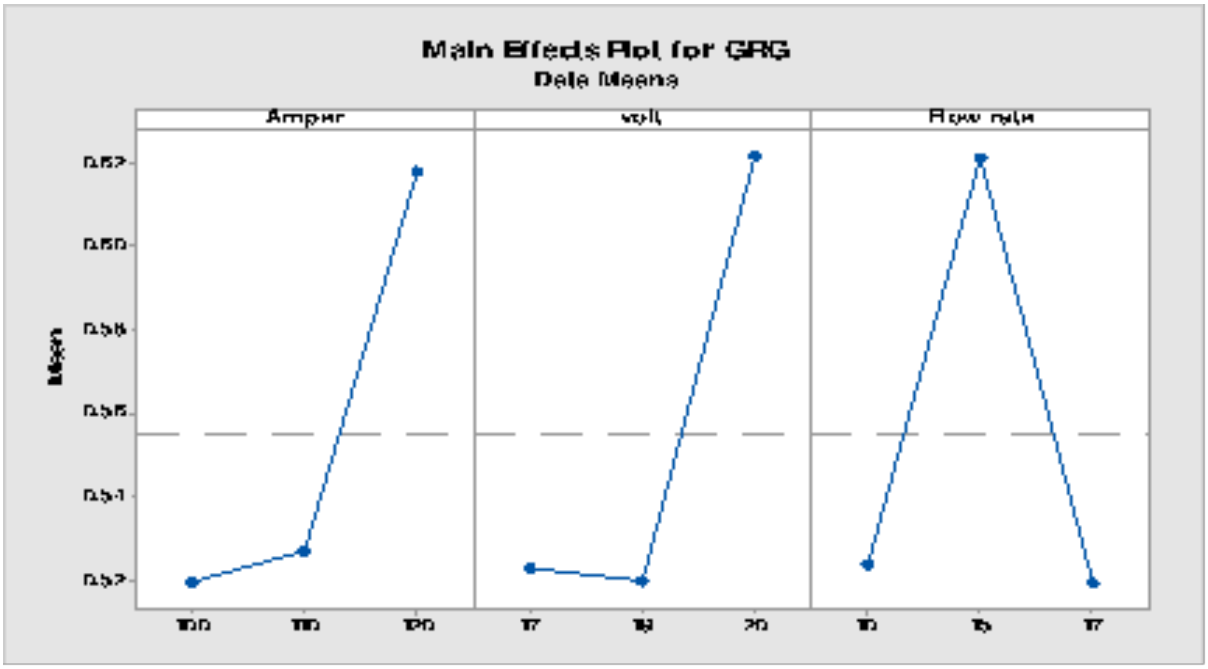

Fig. 10. The grey-relational grade's main effect plot in connection to the input process parameters

That equates to A at level 3 (120 ampers), V at level 3 (20 V), and F at level 2 (15 L/min). The most crucial variable for the multi-performance characteristics was determined using an analysis of variance (ANOVA) with a 95% confidence level, as shown in Table 14. The ANOVA results and their p-values, all less than 0.05%, show that all process parameters were significant. The most significant process parameter, as determined by the p-value test, was voltage, which contributed 65.66% and had a p-value of 0.001. With p-values of 0.05 and 0.04, A and F placed second and third, respectively.

Table 14
The GRG's ANOVA results

Source	DF	Adj S.S.	Contribution	Adj MS	F-Value	P-Value
A	2	0.01812	29.11%	0.009062	0.95	0.0513
V	2	0.02030	65.66%	0.010149	1.06	0.0485
F	2	0.02030	4.01%	0.010006	1.05	0.0489
Error	2	0.01911	1.2%	0.009556		
Total	8	0.07755	100.00%			

4.6 A Verification Test

To verify the multi-performance characteristics' optimization, a confirmatory test was run using the ideal configuration discovered using the grey-based Taguchi approach [22] UTS, VHN, and C.R. measurements of 190.169 MPa, 77.7709 HV, and 0.029 mm, respectively, were achieved with the welding input process parameters set to their ideal values (Aof 120 amper, V of 19, and Fe of 15 L/min). These values are all greater than those obtained from the parameters' original settings, which supports the validity of the TIG welding process's grey-based Taguchi multi-performance characteristics optimization shown in Figure 11.

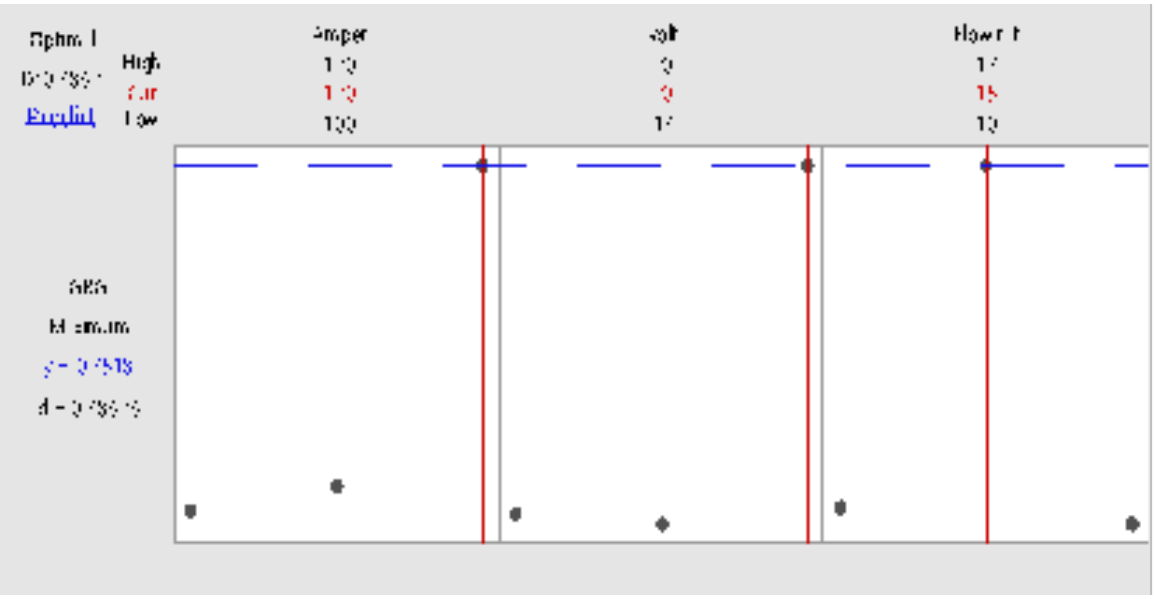

Fig. 11. Utilizing the response optimizer in ANOVA, optimize the variables and responses

5. Conclusions

This work successfully optimized multiple performance aspects, and the TIG welding process was set up to its ideal configuration. Concerning optimizing TIG welding of aluminium 6061, the following conclusions have been made:

i. The best conditions for TIG welding aluminium 6061 using the grey-based Taguchi multi-performance attributes optimization approach are 120 A of welding current, 20 V of welding voltage, and 15 L/min of gas flow.
ii. At the ideal condition, 190.169 MPa of tensile strength, 77.7709 HV of hardness, and 0.029 mm of corrosion rate were reached.
iii. Voltage is the most critical process parameter among those taken into account, contributing 65.66%.
iv. As the voltage rises, the welds' tensile strength rises as well.
v. The corrosion rate of the welds decreases as the voltage rises to 20 v.
vi. The confirmatory test's findings support the optimization procedure.

Acknowledgement
This research was not funded by any grant.

References
[1] Ahmad, Asif, and Shahnawaj Alam. "Integration of RSM with grey based Taguchi method for optimization of pulsed TIG welding process parameters." *Materials today: proceedings* 18 (2019): 5114-5127. https://doi.org/10.1016/j.matpr.2019.07.508
[2] Kumar, Kamlesh, Ch Sateesh Kumar, Manoj Masanta, and Swastik Pradhan. "A review on TIG welding technology variants and its effect on weld geometry." *Materials Today: Proceedings* 50 (2022): 999-1004. https://doi.org/10.1016/j.matpr.2021.07.308
[3] Baskutis, Saulius, Jolanta Baskutiene, Regita Bendikiene, and Antanas Ciuplys. "Effect of weld parameters on mechanical properties and tensile behavior of tungsten inert gas welded AW6082-T6 aluminium alloy." *Journal of Mechanical Science and Technology* 33 (2019): 765-772. https://doi.org/10.1007/s12206-019-0131-6
[4] Liu, L. "Welding and joining of magnesium alloys to aluminum alloys." In *Welding and Joining of Magnesium Alloys*, pp. 38-63e. Woodhead Publishing, 2010. https://doi.org/10.1533/9780857090423.1.38

[5] Devanathan, R., Sanjivi Arul, T. Venkatamuni, D. Yuvarajan, and D. Christopher Selvam. "The effect of sub-zero treatment on mechanical properties of gtaw welded AA6082." *Applied Mechanics and Materials* 852 (2016): 349-354. https://doi.org/10.4028/www.scientific.net/AMM.852.349

[6] Baskutis, Saulius, Jolanta Baskutiene, and Edvinas Bernotaitis. "Experimental study of welded joints of aluminium alloy AW6082." *Solid State Phenomena* 260 (2017): 212-218. https://doi.org/10.4028/www.scientific.net/SSP.260.212

[7] Biswas, Ajay, and Abhijit Bhowmik. "Study of heat generation and its effect during submerged arc welding (SAW) on mild steel plate at zero degree Celsius plate temperature." *Materials Today: Proceedings* 5, no. 5 (2018): 13400-13405. https://doi.org/10.1016/j.matpr.2018.02.333

[8] Rioja, Roberto J., and John Liu. "The evolution of Al-Li base products for aerospace and space applications." *Metallurgical and Materials Transactions A* 43, no. 9 (2012): 3325-3337. https://doi.org/10.1007/s11661-012-1155-z

[9] Xu, Yanling, Gu Fang, Na Lv, Shanben Chen, and Ju Jia Zou. "Computer vision technology for seam tracking in robotic GTAW and GMAW." *Robotics and computer-integrated manufacturing* 32 (2015): 25-36. https://doi.org/10.1016/j.rcim.2014.09.002

[10] Durgutlu, Ahmet. "Experimental investigation of the effect of hydrogen in argon as a shielding gas on TIG welding of austenitic stainless steel." *Materials & design* 25, no. 1 (2004): 19-23. https://doi.org/10.1016/j.matdes.2003.07.004

[11] Sharma, Gaurav, Rohan Tyagi, and Pratishtha Sharma. "Variants of TIG welding process for improvement of weld penetration depth-a review." *Materials Today: Proceedings* 64 (2022): 1362-1366. https://doi.org/10.1016/j.matpr.2022.04.266

[12] Praveen, V. V., T. D. John, and K. M. Peethambaran. "Experimental investigation of welding parameters on automatic TIG welding of aluminium 5083 plate." In *Materials Science Forum*, vol. 879, pp. 1459-1464. Trans Tech Publications Ltd, 2017. https://doi.org/10.4028/www.scientific.net/MSF.879.1459

[13] Sivanantham, A., S. Manivannan, and SP Kumaresh Babu. "Parametric optimization of dissimilar TIG welding of AISI 304L and 430 steel using Taguchi analysis." In *Materials Science Forum*, vol. 969, pp. 625-630. Trans Tech Publications Ltd, 2019. https://doi.org/10.4028/www.scientific.net/MSF.969.625

[14] Dey, Dipankar, Abhijit Bhowmik, and Ajay Biswas. "Tribological performance Optimization of Al2024-TiB2 composites using Grey-Taguchi approach." *International Journal of Cast Metals Research* 35, no. 5-6 (2022): 144-151. https://doi.org/10.1080/13640461.2022.2149361

[15] Dey, Dipankar, Abhijit Bhowmik, and Ajay Biswas. "A grey-fuzzy based multi-response optimisation study on the friction and wear characteristics of titanium diboride reinforced aluminium matrix composite." *Proceedings of the Institution of Mechanical Engineers, Part B: Journal of Engineering Manufacture* (2023): 09544054221147973. https://doi.org/10.1177/09544054221147973

[16] Prajapati, Vishalkumar, Jay J. Vora, Subhash Das, and Kumar Abhishek. "Study of parametric influence and welding performance optimization during regulated metal deposition (RMD™) using grey integrated with fuzzy taguchi approach." *Journal of Manufacturing Processes* 54 (2020): 286-300. https://doi.org/10.1016/j.jmapro.2020.03.017

[17] Mahbubah, N. A., M. Nuruddin, S. S. Dahda, D. Andesta, E. Ismiyah, D. Widyaningrum, M. Z. Fathoni *et al.,* "Optimization of CNC Turning Parameters for cutting Al6061 to Achieve Good Surface Roughness Based on Taguchi Method." *Journal of Advanced Research in Applied Mechanics* 99, no. 1 (2022): 1-9.

[18] Huang, Lijin, Xueming Hua, Dongsheng Wu, Zhao Jiang, and Youxiong Ye. "A study on the metallurgical and mechanical properties of a GMAW-welded Al-Mg alloy with different plate thicknesses." *Journal of Manufacturing Processes* 37 (2019): 438-445. https://doi.org/10.1016/j.jmapro.2018.12.017

[19] Benakis, Michalis, Davide Costanzo, and Alin Patran. "Current mode effects on weld bead geometry and heat affected zone in pulsed wire arc additive manufacturing of Ti-6-4 and Inconel 718." *Journal of Manufacturing Processes* 60 (2020): 61-74. https://doi.org/10.1016/j.jmapro.2020.10.018

[20] Ingle, Avinash Ishwer, H. D. Shashikala, Manoj Kumar Narayanan, Mathewos Tulore Dubeto, and Shubham Gupta. "Optimization and analysis of process parameters of melt quenching technique for multiple performances of rare earth doped barium borate glass synthesis using Taguchi's design and grey relational approach." *Results in Engineering* 17 (2023): 100784. https://doi.org/10.1016/j.rineng.2022.100784

[21] Gul, M., M. A. Kalam, M. A. Mujtaba, Saira Alam, M. Nasir Bashir, Iqra Javed, Umair Aziz, M. Rizwan Farid, M. Tahir Hassan, and Shahid Iqbal. "Multi-objective-optimization of process parameters of industrial-gas-turbine fueled with natural gas by using Grey-Taguchi and ANN methods for better performance." *Energy Reports* 6 (2020): 2394-2402. https://doi.org/10.1016/j.egyr.2020.08.002

[22] Ahmad, Asif, and Shahnawaj Alam. "Integration of RSM with grey based Taguchi method for optimization of pulsed TIG welding process parameters." *Materials today: proceedings* 18 (2019): 5114-5127. https://doi.org/10.1016/j.matpr.2019.07.508

[23] Sabry, Ibrahim, Amir Hussain Idrisi, and Abdel Hamid Ismail Mourad. "Friction stir welding process parameters optimization through hybrid multi-criteria decision-making approach." *International Review on Modelling and Simulations* 14, no. 1 (2021): 32-43. https://doi.org/10.15866/iremos.v14i1.19537

[24] Kim, Hang Rae, Young Woo Park, and Kang Yong Lee. "Application of grey relational analysis to determine welding parameters for Nd: YAG laser GMA hybrid welding of aluminium alloy." *Science and Technology of Welding and Joining* 13, no. 4 (2008): 312-317. https://doi.org/10.1179/174329307X249423

[25] Sabry, Ibrahim, Dinu Thomas Thekkuden, Abdel-Hamid I. Mourad, and Sanan Husain Khan. "Optimization of tungsten inert gas welding parameters using grey relational analysis for joining AA 6082 pipes." In *2022 Advances in Science and Engineering Technology International Conferences (ASET)*, pp. 1-6. IEEE, 2022. https://doi.org/10.1109/ASET53988.2022.9735100

[26] Sabry, Ibrahim, Dinu Thomas Thekkuden, and Abdel-Hamid I. Mourad. "TOPSIS–GRA approach to optimize friction stir welded aluminum 6061 pipes parameters." In *2022 Advances in Science and Engineering Technology International Conferences (ASET)*, pp. 1-6. IEEE, 2022. https://doi.org/10.1109/ASET53988.2022.9734821

[27] Suji, D., Adeyemi Adesina, and R. Mirdula. "Optimization of self-compacting composite composition using Taguchi-Grey relational analysis." *Materialia* 15 (2021): 101027. https://doi.org/10.1016/j.mtla.2021.101027

[28] Sabry, Ibrahim, Abdel-Hamid I. Mourad, and Dinu Thomas Thekkuden. "Optimization of metal inert gas-welded aluminium 6061 pipe parameters using analysis of variance and grey relational analysis." *SN Applied Sciences* 2 (2020): 1-11. https://doi.org/10.1007/s42452-020-1943-9

[29] Sivasakthivel, P. S., and R. Sudhakaran. "Modelling and optimisation of welding parameters for multiple objectives in pre-heated gas metal arc welding process using nature instigated algorithms." *Australian Journal of Mechanical Engineering* (2018). https://doi.org/10.1080/14484846.2018.1472721